Sensors and Materials, Vol. 37, No. 9 (2025) 3881–3892
MYU Tokyo

S & M 4159

Anomaly Flying Height Prediction Based on Clustering Techniques in Hard Disk Drive Manufacturing

Worawit Kanjanapruthipong[1] and Poom Konghuayrob[2*]

[1]Department of Robotics and AI Engineering, School of Engineering, King Mongkut's Institute of Technology Ladkrabang, 1, Soi Chalong Krung 1, Ladkrabang, Bangkok 10520, Thailand
[2]Department of Electrical Engineering, School of Engineering, King Mongkut's Institute of Technology Ladkrabang, 1, Soi Chalong Krung 1, Ladkrabang, Bangkok 10520, Thailand

(Received June 30, 2025; accepted August 4, 2025)

Keywords: flying height, hard disk drive, AI, clustering, KMeans, MiniBatchKMeans, Birch, BisectingKMeans, Elbow method, confusion matrix, mosaic plot

In this research, we present a method for predicting anomaly flying height (FH) profiles in hard disk drive (HDD) manufacturing by analyzing FH data at the FH1 stage. Anomalies at FH1 can lead to calibration issues at FH2, disrupting the production process. We propose an AI-based approach using unsupervised clustering techniques to group FH profiles of the read/write head. We evaluated four clustering algorithms, KMeans, MiniBatchKMeans, Birch, and BisectingKMeans, along with the Elbow method to determine the optimal number of clusters. By identifying anomalous FH profiles early at FH1, the method enables proactive intervention, reducing calibration process time and improving production efficiency. Our model achieved an accuracy of 0.939 without relying on manual feature selection (e.g., pressure and temperature), which is often difficult to capture using traditional linear or rule-based models owing to the nonlinear nature of FH profiles. These results demonstrate the practical potential of clustering techniques in enhancing HDD manufacturing processes.

1. Introduction

Flying height (FH) calibration is a critical process in hard disk drive (HDD) manufacturing. It involves heating a coil element with electric current to induce the protrusion of the read/write head until it reaches the target FH, the clearance between the head and the disk surface. This protrusion, controlled by HDD firmware and preamp hardware, is converted from digital-to-analog converter (DAC) units to milliwatts to ensure optimal read/write performance. Multiple FH calibration stages are performed throughout the manufacturing process to meet quality and standardization requirements. However, anomalies in FH calibration can occasionally occur. These anomalies are reflected in the FH profile, reported in DAC units across the disk surface, and divided into 240 zones per head. Modern HDDs can have up to 20 read/write heads, each

*Corresponding author: e-mail: poom.ko@kmitl.ac.th
https://doi.org/10.18494/SAM5832

ISSN 0914-4935
https://myukk.org/

flying independently. In this study, we focus on two key calibration stages, FH1 and FH2, as shown in Fig. 1.

Previous research has explored physics-based approaches to improve FH calibration.[1–3] Juang *et al.*[4] modeled nonlinear FH protrusion under varying environmental conditions. Boettcher *et al.*[5] proposed a dynamic FH model with feedforward control to reduce variation. Abdevand *et al.*[6] developed an analog circuit (ASIC) using FH sensors to measure head-to-disk distance, enhancing storage capacity. While these studies aimed to optimize FH profiles, they did not incorporate AI techniques. In 2024, Kanjanapruthipong *et al.*[7] introduced an AI-based method for FH calibration, predicting FH profiles in DAC units and significantly reducing calibration time.

Building on this, we addressed anomalies caused by mechanical interference and unexpected head deformation, as shown in Fig. 2, which directly impact FH calibration and DAC profiles. We propose an unsupervised learning approach using clustering techniques, KMeans,[8–13] MiniBatchKMeans,[14] Birch,[15] and BisectingKMeans,[16] combined with the Elbow method[17,18] to determine the optimal number of clusters. This method enables the early detection of anomalous FH profiles at FH1, preventing defective drives from proceeding to FH2, thereby improving calibration efficiency.

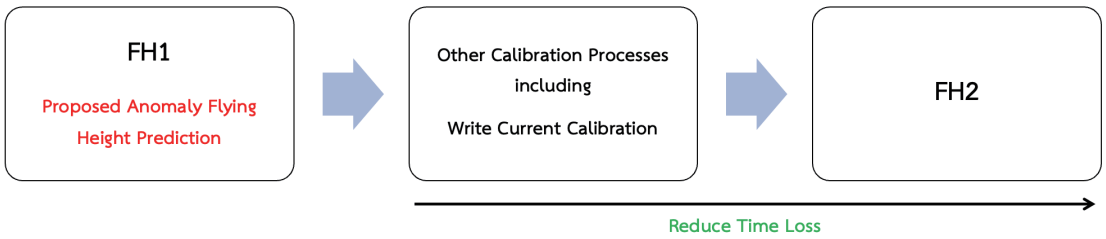

Fig. 1. (Color online) Overview of FH calibration and the proposed anomaly FH prediction method designed to reduce time loss related to potential issues.

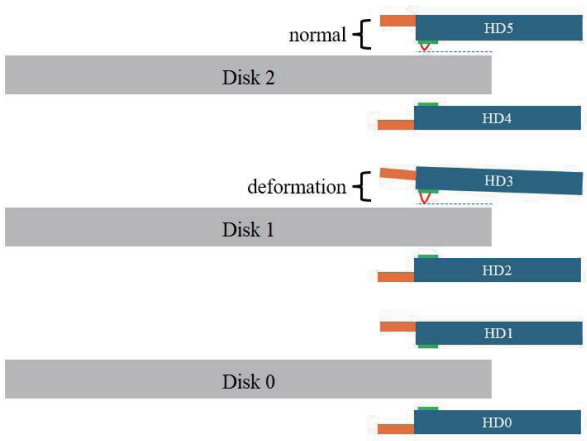

Fig. 2. (Color online) Illustration of an anomalous read/write head exhibiting unexpected deformation.

2. Experimental Procedure

2.1 Points of interest in FH calibration

Kanjanapruthipong *et al.*[7] investigated the calibration of FH in HDDs by analyzing the protrusion value of the read/write head, expressed in DAC units. This value represents the distance from the tip of the head to the target FH position, referred to as point B. The distance labeled A, known as thermal protrusion, was modeled and predicted through experimental analysis. As shown in Fig. 3 (reproduced from Ref. 7 under CC BY 4.0 License. https://doi.org/10.18494/SAM4825), the thermal protrusion (distance A) at FH1 across each zone is used as input to predict the corresponding value at FH2. This relationship forms the basis of the current study, which aims to apply clustering techniques to classify early anomalies in FH profiles at FH1. By identifying these anomalies early, the method can prevent defective drives from proceeding to FH2, thereby improving calibration efficiency.

2.2 Analysis of FH calibration patterns

An analysis of the DAC profiles from FH calibration revealed distinct differences between unhealthy and healthy read/write heads. In HDDs where certain heads were unhealthy to proceed to FH2, the FH1 DAC profiles exhibited significant deviations compared with those of functional heads. As shown in Fig. 4, the blue line represents the DAC profile of an unhealthy head, whereas the red line shows a typical profile from a healthy head. These anomalies are clearly observable at the FH1 stage, indicating the potential for early detection.

2.3 Data preparation

The training dataset was constructed using data from 44 HDDs, each containing 20 read/write heads and 240 zones per head, resulting in a total of 211200 data points (44 × 20 × 240). Among these, 58 read/write heads were identified as unhealthy, whereas 822 were classified as healthy. Each data sample consists of 240 features, corresponding to the DAC values across all zones for a single head at the FH1 stage. These FH1 DAC profiles, representing both unhealthy

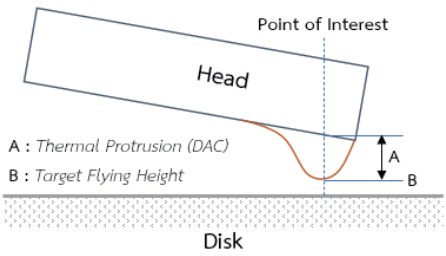

Fig. 3. (Color online) Key points of interest on the read/write head relevant to FH calibration.[7]

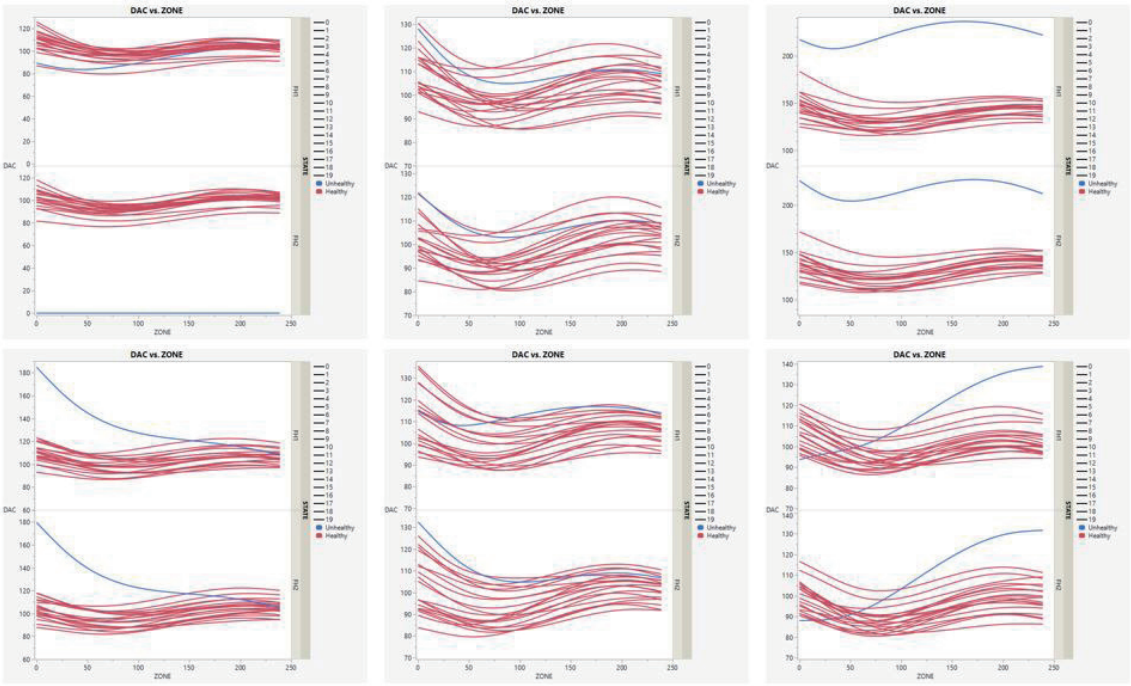

Fig. 4. (Color online) Examples of unhealthy (blue lines) and healthy (red lines) patterns observed during FH1 (upper panel) and FH2 (lower panel) calibration stages for selected read/write heads.

and healthy heads, were used as input to the clustering model. The model's objective was to group the profiles into clusters that reflect distinct calibration patterns, enabling the identification of anomalous profiles associated with potential issues.

2.4 Clustering techniques and evaluation criteria

In this study, we propose an AI-based approach for predicting anomaly FH profiles at FH1 using clustering algorithms suitable for unsupervised learning. The focus is on four clustering methods, KMeans, MiniBatchKMeans, Birch, and BisectingKMeans, with the Elbow method employed to determine the optimal number of clusters.

KMeans is a popular unsupervised learning algorithm that divides data into k clusters, each consisting of the most similar data. This algorithm iteratively alternates between assigning points to the nearest cluster and updating cluster centroids until the result convergence. KMeans aims to find the value that minimizes the total distance within clusters, as shown in Eqs. (1) and (2), also known as the Within-Cluster Sum of Squares (WCSS).

MiniBatchKMeans is a scalable variant of KMeans that updates cluster centroids incrementally using small random subsets of the data. This reduces computational cost and memory usage while maintaining clustering performance similar to standard KMeans.

Birch is a hierarchical clustering method that builds a compact Clustering Feature tree from the input data. It incrementally clusters incoming samples using threshold-based criteria and is particularly effective for large datasets owing to its low memory usage and high efficiency.

BisectingKMeans applies KMeans with $k = 2$ to partition the dataset into two subgroups, often resulting in better-separated clusters than standard KMeans.

The Elbow method is a technique to find the optimal number of clusters k by measuring the WCSS and looking for the point at which the error decays more slowly, like the elbow of an arm. The WCSS function helps measure the compactness of the clusters by summing the squared distances between each data point and the centroid of its assigned cluster, as shown in Eq. (3). The Elbow method can run KMeans, MiniBatchKMeans, Birch, and BisectingKMeans for various values of k, and calculate the WCSS for each k, then plot the WCSS against k and find the Elbow point, which is the point at which the WCSS begins to decay more slowly. This allows us to calculate the rate at which the WCSS changes between different values of k and find the Elbow point, as shown in Eq. (4). Therefore, a lower WCSS means that the cluster is compact and well organized.

KMeans objective function:

$$\underset{C}{\operatorname{argmin}} \sum_{i=1}^{k} \sum_{x \in C_i} \left\| x - \mu_i \right\|^2 \tag{1}$$

$$\mu_i = \frac{1}{|C_i|} \sum_{x \in C_i} x \tag{2}$$

WCSS:

$$WCSS(k) = \sum_{i=1}^{k} \sum_{x \in C_i} \left\| x - \mu_i \right\|^2 \tag{3}$$

$$\Delta WCSS = WCSS(k) - WCSS(k+1) \tag{4}$$

Here, k is the number of clusters, C_i is the ith cluster, μ_i is the centroid of the cluster C_i, x is each data point, and $||x - \mu_i||^2$ is the squared distance between the data x and the centroid of the cluster. Each centroid μ_i is updated as the mean of the points in its cluster.

A confusion matrix is a table for evaluating the performance of a model that performs classification tasks by showing the number of values the model correctly and incorrectly predicts. A 2 × 2 confusion matrix for a two-class classification problem (binary classification) describes that true positive (TP) predicts positive and is positive, false negative (FN) predicts negative but is positive, false positive (FP) predicts positive but is negative, and true negative (TN) predicts negative and is negative. These values can be used to calculate important statistical values such as accuracy (overall accuracy) as shown in Eq. (5), precision (prediction accuracy of positive) as shown in Eq. (6), recall or sensitivity (the ability to correctly identify positive cases) as shown in Eq. (7), and F1-score (average between precision and recall) as shown in Eq. (8).

Accuracy:

$$Accuracy = \frac{TP + TN}{TP + TN + FP + FN} \tag{5}$$

Precision:

$$Precision = \frac{TP}{TP + FP} \tag{6}$$

Recall or Sensitivity:

$$Recall = \frac{TP}{TP + FN} \tag{7}$$

F1-score:

$$F1\text{-}score = \frac{2 \times Precision \times Recall}{Precision + Recall} \tag{8}$$

3. Results and Discussion

3.1 Exploratory experiments with cluster-k values

To explore the effectiveness of clustering in identifying anomalous FH profiles, we conducted experiments using the KMeans algorithm with different values of k (3, 5, and 7). The goal was to observe how well the clusters correspond to known unhealthy and healthy read/write heads, as determined through the physical analysis of HDDs. A Mosaic plot was used to visualize the relationship between the clustering results and the actual status. In these plots, each bar represents the frequency of read/write heads assigned to a particular cluster. The color coding distinguishes between unhealthy (red) and healthy (blue) heads. The x-axis represents the cluster labels generated by KMeans. As shown in Fig. 5, the left, middle, and right plots correspond to k values of 3, 5, and 7, respectively. Clusters with a high proportion of red bars indicate groups where unhealthy heads are concentrated. These clusters are considered effective in identifying anomalous FH profiles at the FH1 stage.

After identifying the target groups through clustering, the performance of the model in predicting outcomes during FH calibration was evaluated using a confusion matrix. The results revealed varying levels of accuracy depending on the number of clusters used in the KMeans algorithm. Specifically, clustering with $k = 3$ yielded an accuracy of 0.545, while $k = 5$ resulted in a slightly lower accuracy of 0.508. Notably, clustering with $k = 7$ achieved a significantly higher accuracy of 0.753, as shown in Fig. 6. These findings suggest that increasing the number

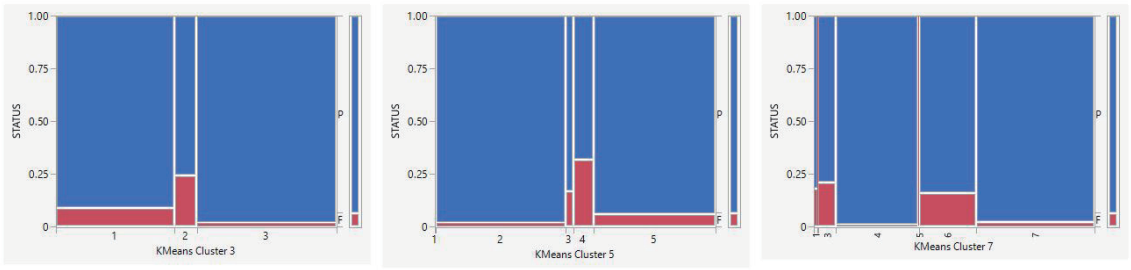

(a) (b) (c)

Fig. 5. (Color online) Mosaic plots showing the relationship between unhealthy and healthy read/write heads across KMeans clustering results: (a) $k = 3$, (b) $k = 5$, and (c) $k = 7$.

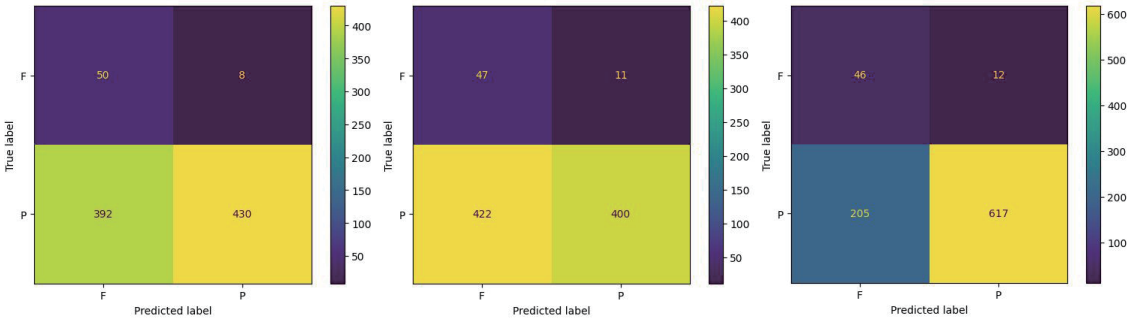

(a) (b) (c)

Fig. 6. (Color online) Experimental results of KMeans clustering: (a) $k = 3$, accuracy = 0.545; (b) $k = 5$, accuracy = 0.508; (c) $k = 7$, accuracy = 0.753.

of clusters can enhance the model's ability to distinguish between unhealthy and healthy read/write heads, although the choice of k must balance granularity with generalization.

3.2 Applying the Elbow method to determine the optimal cluster-k experiment

After observing that using arbitrary values of k (such as 3, 5, and 7) resulted in suboptimal prediction accuracy, we applied the Elbow method to identify the most appropriate number of clusters. The Elbow method is a widely used technique for determining the optimal k by analyzing the rate of change in WCSS. To enhance the robustness of the analysis, the experiment was extended to include several commonly used clustering algorithms: KMeans, MiniBatchKMeans, Birch, and BisectingKMeans. The initial parameters of those algorithms are presented in Table 1. The Elbow method was applied to each algorithm to evaluate the consistency of the optimal cluster count across different techniques. The results showed that all four algorithms suggested a similar optimal number of clusters, approximately $k = 10$. This consistency reinforces the reliability of the Elbow method in this context. The relationship between the number of clusters (k) and the WCSS for each algorithm is shown in Fig. 7. At $k = 1$, the WCSS is notably high. As k increases, the WCSS decreases steadily. The "elbow" point, defined as the point at which the rate of decrease in WCSS begins to slow, indicates the most suitable value of k for effective clustering.

Table 1
Initial parameters of KMeans, MiniBatchKMeans, Birch, and BisectingKMeans used in the Elbow method.

Model	n_clusters (k) used in the elbow method	init	n_init	max_iter	tol	Other key parameters
KMeans	1 - 30	k-means++	auto	300	0.0001	algorithm = 'lloyd'
MiniBatchKMeans	1 - 30	k-means++	auto	100	0.0	batch_size = 1024, reassignment_ratio = 0.01
Birch	1 - 30	–	–	–	–	threshold = 0.5, branching_factor = 50
BisectingKMeans	1 - 30	k-means++	auto	300	0.0001	–

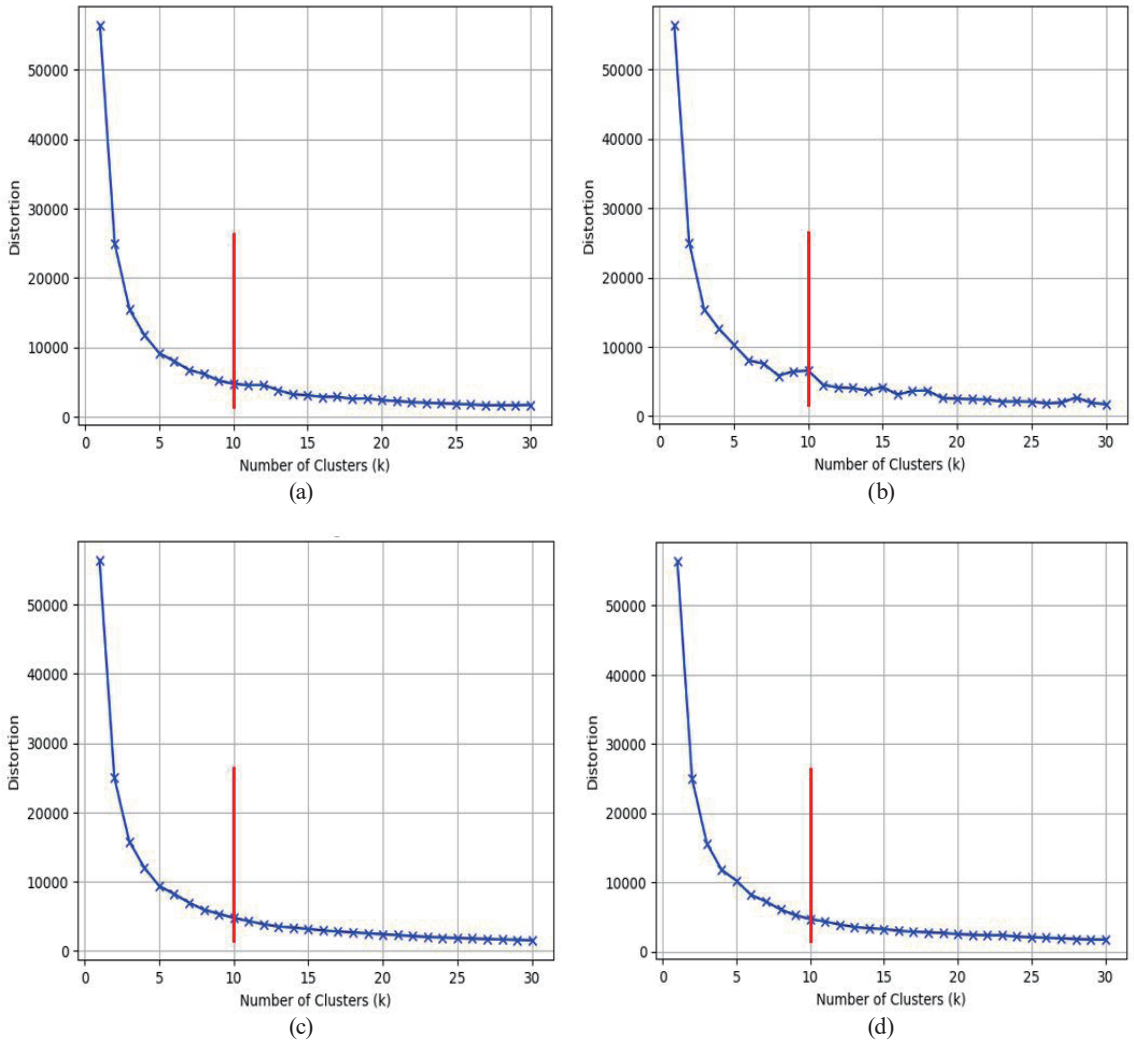

Fig. 7. (Color online) Elbow method using distortion plots for determining optimal number of clusters (k): (a) KMeans, (b) MiniBatchKMeans, (c) Birch, and (d) BisectingKMeans.

After determining the optimal number of clusters, $k = 10$, across all four clustering models, a Mosaic plot was employed to visualize the relationship between confirmed unhealthy and healthy read/write heads. This visualization was then compared with the clustering results from KMeans, MiniBatchKMeans, Birch, and BisectingKMeans. As shown in Fig. 8, red bars represent unhealthy read/write heads, whereas blue bars indicate healthy ones. The x-axis denotes the cluster indices generated by each clustering algorithm. Clusters characterized by prominently tall red bars were identified as those most indicative of read/write heads likely to be unhealthy during the FH calibration.

After identifying the target group through the prediction method applied during the FH calibration of the read/write head, the results were reevaluated using a confusion matrix. The findings demonstrated that the Elbow method provided satisfactory experimental outcomes with high accuracy across all models. Specifically, KMeans achieved an accuracy of 0.939, MiniBatchKMeans 0.914, Birch 0.915, and BisectingKMeans 0.910, as shown in Fig. 9. A detailed comparison of the experimental results and statistical performance of the four clustering algorithms, based on the Elbow method, and additional exploratory experiments using KMeans with varying cluster values (k) are presented in Table 2.

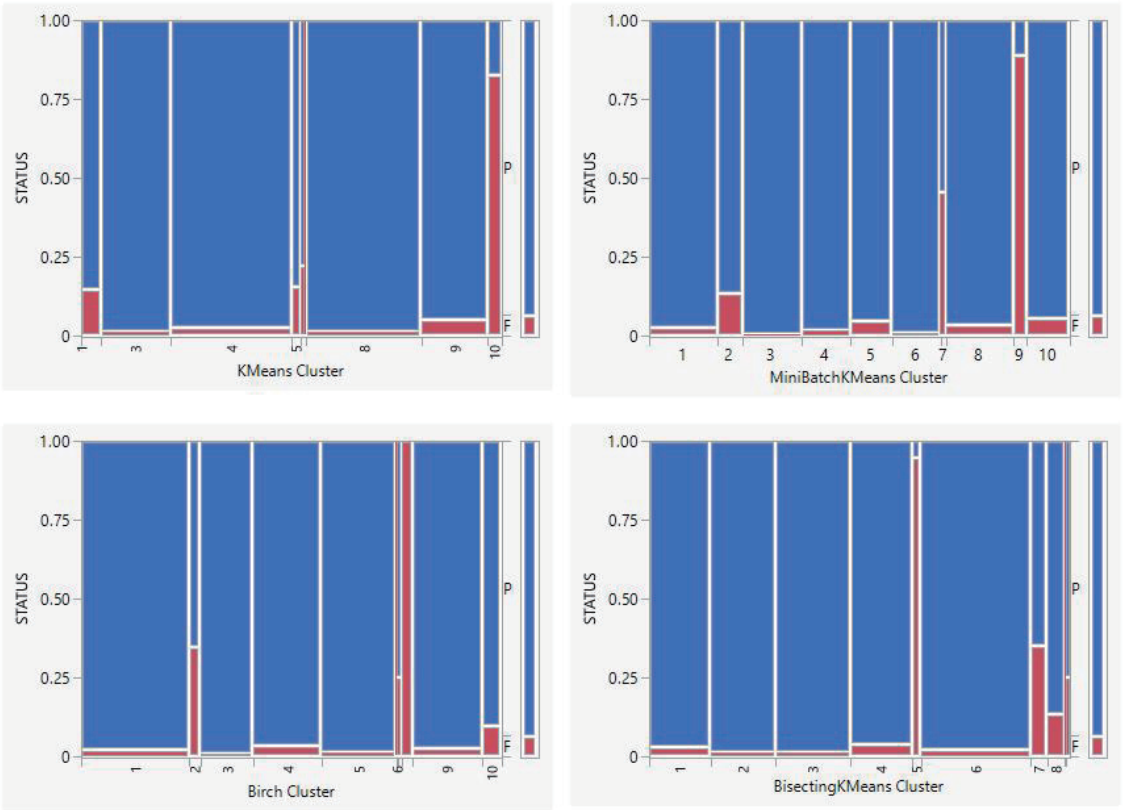

Fig. 8. (Color online) Mosaic plots comparing unhealthy and healthy read/write heads across clusters generated by the four clustering algorithms.

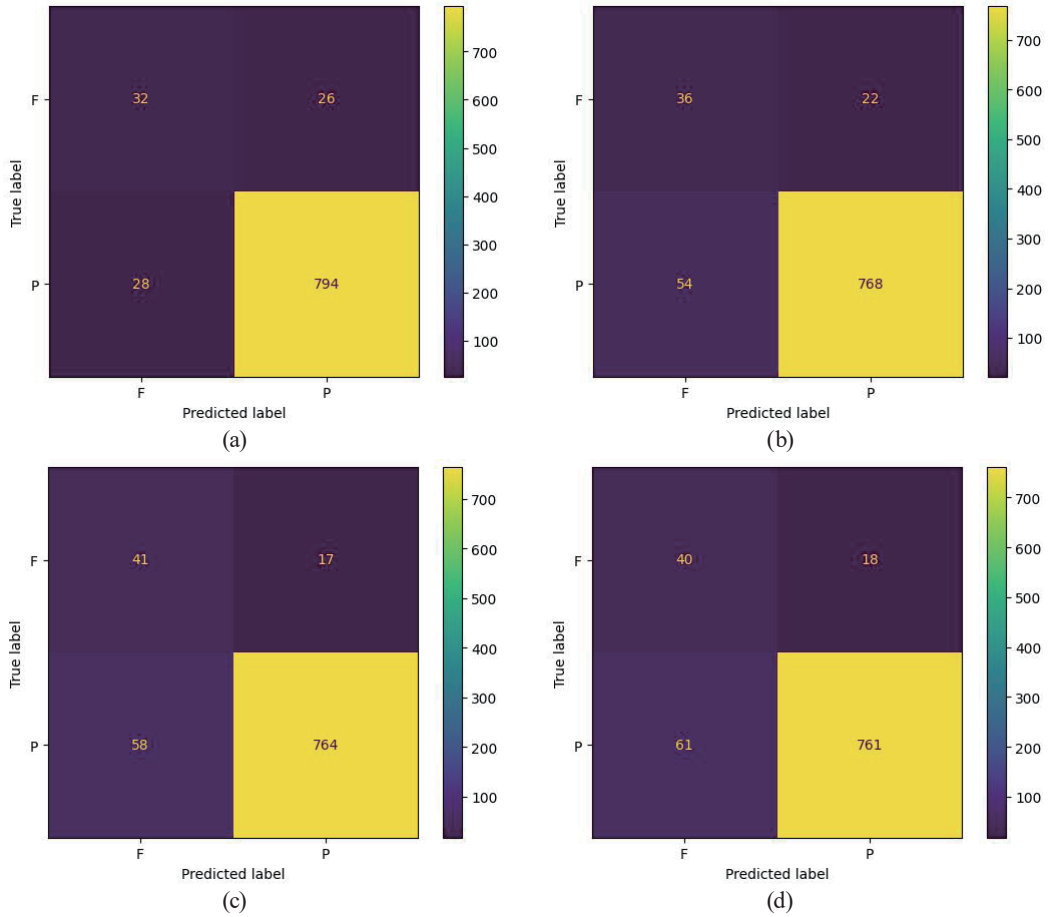

Fig. 9. (Color online) Accuracy results of the four clustering algorithms: (a) KMeans (0.939), (b) MiniBatchKMeans (0.914), (c) Birch (0.915), and (d) BisectingKMeans (0.910).

Table 2
Experimental results and statistical performance of the four clustering algorithms using the Elbow method, including exploratory experiments with KMeans at varying cluster values.

Model	Elbow method	Cluster-k	*TP–FN–FP–TN*	Accuracy	Precision	Sensitivity	F1-score
KMeans	yes	10	794–28–26–32	0.939	0.968	0.966	0.967
MiniBatchKMeans	yes	10	768–54–22–36	0.914	0.972	0.934	0.953
Birch	yes	10	764–58–17–41	0.915	0.978	0.929	0.953
BisectingKMeans	yes	10	761–61–18–40	0.910	0.977	0.926	0.951
KMeans	no	3	430–392–8–50	0.545	0.982	0.523	0.683
KMeans	no	5	400–422–11–47	0.508	0.973	0.487	0.649
KMeans	no	7	617–205–12–46	0.753	0.981	0.751	0.850

After completing the clustering-based prediction process, a graph was generated to visualize the grouping of FH DAC profiles, highlighting anomalous profiles of the read/write heads. The results demonstrated consistent and satisfactory performance across all four clustering algorithms. As shown in Fig. 10, solid-colored lines represent clusters associated with anomalous

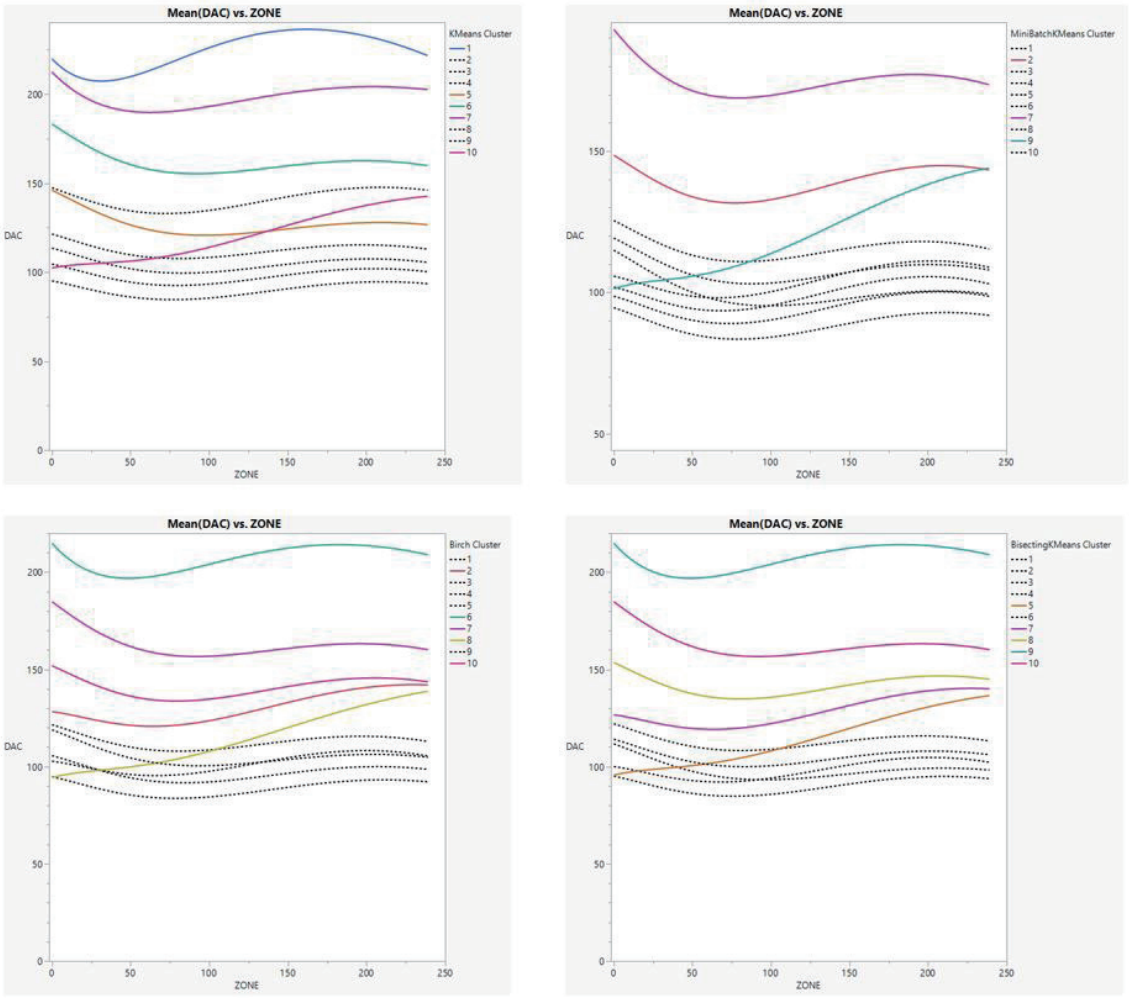

Fig. 10. (Color online) Visualization of FH DAC profile clustering, showing both anomalous and normal FH profiles across all four clustering algorithms.

FH profiles, whereas the dashed black line denotes the cluster corresponding to normal FH profiles.

4. Conclusions

In this study, we investigated the anomaly detection in the FH calibration of read/write heads and proposed a method for predicting anomalous FH profiles in HDDs using clustering techniques combined with the Elbow method, which determines the optimal number of clusters for the dataset. The four clustering algorithms, KMeans, MiniBatchKMeans, Birch, and BisectingKMeans, demonstrated satisfactory performance, with the highest accuracy reaching 0.939 and an F1-score of 0.967. These results indicate that the model effectively identifies true anomalies while minimizing false positives. The proposed approach is well suited for integration into AI-driven manufacturing systems. It enables the early detection and classification of

anomalies in FH profiles at the FH1 stage. Consequently, HDDs identified with potential issues can be excluded from subsequent production steps, such as FH2 calibration. This proactive filtering not only prevents unnecessary calibration attempts likely to become unhealthy but also enhances the overall efficiency and reliability of the FH calibration process.

Acknowledgments

For industrial purposes, this research was supported by funding from the School of Engineering, King Mongkut's Institute of Technology Ladkrabang.

References

1 H. Dakroub, M. C. Rao, and A. G. Sam: "Fly Height Measurement for A Disc Drive," US Patent: US6898034, Assignee: Seagate Technology LLC, Publication date on May 24, 2005. https://patents.google.com/patent/US6898034B2/en (accessed June 2025).
2 B. C. Schardt, E. Schreck, R. Sonnenfeld, Q. Haddock, and J. R. Haggis: IEEE Trans. Magn. **34** (1998) 1765. https://doi.org/10.1109/20.706699
3 V. J. Novotny: IEEE Trans. Magn. **33** (1997) 3115. https://doi.org/10.1109/20.617862
4 J. Y. Juang, T. Nakamura, B. Knigge, Y. Luo, W. C. Hsiao, K. Kuroki, F. Y. Huang, and P. Baumgart: IEEE Trans. Magn. **44** (2008) 3679. https://doi.org/10.1109/TMAG.2008.2002612
5 U. Boettcher, H. Li, R. A. de Callafon, and F. E. Talke: IEEE Trans. Magn. **47** (2011) 1823. https://doi.org/10.1109/TMAG.2011.2136328
6 M. M. Abdevand, D. Livornesi, A. E. Vergani, F. Piscitelli, E. Mammei, E. Bonizzoni, P. Malcovati, and P. Pulici: IEEE Trans. Circuits Syst. I Regul. Pap. **71** (2024) 4458. https://doi.org/10.1109/TCSI.2024.3436034
7 W. Kanjanapruthipong, P. Prasitmeeboon, and P. Konghuayrob: Sens. Mater. **36** (2024) 1377. https://doi.org/10.18494/SAM4825
8 D. Cheng, J. Huang, S. Zhang, S. Xia, G. Wang, and J. Xie: IEEE Trans. Neural Networks Learn. Syst. **35** (2024) 11077. https://doi.org/10.1109/TNNLS.2023.3248064
9 J. Wang and X. Li: IEEE Access. **12** (2024) 99110. https://doi.org/10.1109/ACCESS.2024.3429304
10 A. Mirzal: IEEE/ACM Trans. Comput. Biol. Bioinf. **19** (2022) 1173. https://doi.org/10.1109/TCBB.2020.3025486
11 L. Wei, H. Ma, Y. Yin, and C. Geng: IEEE Access **11** (2023) 26566. https://doi.org/10.1109/ACCESS.2023.3257859
12 M. A. Abusubaih and S. Khamayseh: IEEE Access **10** (2022) 1410. https://doi.org/10.1109/ACCESS.2021.3138888
13 P. W. Khan and Y. C. Byun: IEEE Open Access J. Power Energy **11** (2024) 349. https://doi.org/10.1109/OAJPE.2024.3437414
14 S. C. Hicks, R. Liu, Y. Ni, E. Purdom, and D. Risso: PLoS Comput. Biol. **17** (2021) 1. https://doi.org/10.1371/journal.pcbi.1008625
15 T. Zhang, R. Ramakrishnan, and M. Livny: Data Min. Knowl. Discovery. **1** (1997) 141. https://doi.org/10.1023/A:1009783824328
16 S. Banerjee, A. Choudhary, and S. Pal: 2015 IEEE Int. WIE Conf. Electrical and Computer Engineering (WIECON-ECE) 168–172. https://doi.org/10.1109/WIECON-ECE.2015.7443889
17 G. Racolte, A. Marques, L. Scalco, L. Tonietto, D. C. Zanotta, C. L. Cazarin, L. Gonzaga, and M. R. Veronez: IEEE Access **10** (2022) 63723. https://doi.org/10.1109/ACCESS.2022.3182332
18 L. Zhang, B. Xing, Y. Gao, L. Yao, D. Zhao, J. Ding, and Y. Li: IEEE Access **12** (2024) 183581. https://doi.org/10.1109/ACCESS.2024.3471777